Supplement of

Barium stable isotopes as a fingerprint of biological cycling in the Amazon Basin

Quentin Charbonnier[1,2], Julien Bouchez[1], Jérôme Gaillardet[1,3], and Eric Gayer[1]

[1]Université de Paris, Institut de physique du globe de Paris, CNRS, F-75005 Paris, France
[2]Institute of Geochemistry and Petrology, Department of Earth Sciences, ETH Zürich, Clausiusstrasse 25, 8092 Zürich, Switzerland
[3]Institut Universitaire de France and Université Paris Diderot, Paris, France

Correspondence: Quentin Charbonnier (quentin.charbonnier@erdw.ethz.ch)

1 Supporting text

1.1 Assessing the role of floodplain processes on the river dissolved Ba abundance and isotope composition in the Amazon Basin

As shown by Bouchez et al. (2012) and Dellinger et al. (2015b), the Amazon floodplains are the loci of a range of chemical reactions thought to influence the chemical and isotope composition of the river dissolved load through the alteration of mineral and organic phases. In order to identify possible processes involving Ba within the Amazon floodplains, it is possible to compare the flux of Ba delivered by tributaries upstream from a river reach in the Amazon lowlands where floodplains have developed with that exported downstream from the same reach:

$$\Delta F_{diss}^{Ba} = F_{diss,down}^{Ba} - \Sigma_i F_{diss,up,i}^{Ba} \quad \text{(S.1)}$$

with ΔF_{diss}^{Ba} the shift in river dissolved Ba dissolved flux between $\Sigma_i F_{diss,up,i}^{Ba}$ (the sum of river dissolved Ba inputs to the reach from all upstream tributaries i) and the river dissolved Ba flux downstream from the confluence $F_{diss,down}^{Ba}$. If ΔF_{diss}^{Ba} is equal to 0, the flux of dissolved Ba remains unchanged through the floodplains thereby ruling out floodplain-specific processes affecting Ba. If ΔF_{diss}^{Ba} is positive, dissolved Ba is "produced" by the floodplain (*e.g.* through mineral dissolution or organic matter remineralization); if ΔF_{diss}^{Ba} is negative, dissolved Ba is "consumed" by the floodplains (*e.g.* through the formation of secondary weathering products such as clays or oxides, or through biological uptake).

Dissolved Ba fluxes are calculated using our own measurements of dissolved Ba concentrations and discharge data from long-term river monitoring programs. Data and results are provided in Table S.3 for the few reaches where such calculation can be performed (*i.e.* where the dissolved Ba concentration and discharge are know for all tributaries contributing to the reach, and for the river location downstream from the floodplain reach).

The main result of these calculations is the systematic increase of dissolved Ba fluxes from the Andes to the floodplains, in conjunction with the observed increase in dissolved Ba/Na ratio. We suggest that such relation is driven by the Ba enrichment from "dilute" tributaries which display the highest dissolved Ba/Na ratios. In any case, this analysis dismisses the role of floodplains in scavenging dissolved river Ba and driving Ba isotope fractionation across the transition from the Andes to the plains of the Amazon.

1.2 Gross Primary Production (GPP), Terrestrial Ecosystem Respiration (TER), Mean Annual Precipitation (MAP), and Mean Annual Temperature (MAP) remote sensing data

Catchment-scale values of Gross Primary Production (GPP) and Terrestrial Ecosystem Respiration (TER) of each Amazon tributary under investigation were calculated using data from the " FLUXCOM: http://www.fluxcom.org (RS+METEO) Global Land Carbon Fluxes" data portal (Tramontana et al., 2016; Jung et al., 2019). Catchment-scale MAP and MAT data are derived from https://www.worldclim.org. Annual GPP, TER, MAP and MAT grids of 0.5 degree resolution over the period 1980 to 2013 were stacked to produce one grid with the mean annual value for each of these parameters.

1.3 Re-visiting the Amazon river mass and isotope budgets for Li

Using river mass budgets equations, it is possible to compare the chemical and isotope composition of the river dissolved and solid fluxes with estimates of the supply of material to the Earth surface. Such approach can be applied to reconstruct the composition of the continental crust subjected to denudation, or to check whether the river mass budgets can be qualified as being "at equilibrium" Gaillardet et al. (1995). In the present study, the second application is sought for.

Usually, river mass budgets rely on the use of pairs of elements, expressed as concentration ratios (soluble element over an insoluble element); and the partitioning of isotopes between dissolved and solid compartments during weathering reactions. Dellinger et al. (2015a) applied such a set of river mass and isotope budget equations to Li. The authors showed that in the Amazon the sum of the solid and dissolved Li fluxes exported by rivers, and their combined isotope composition as well, can be accounted for by independent estimate of flux and isotope composition of Li eroded and weathered from rocks. Using the approach detailed in section 4.5 and Appendix C, we can re-visit the data provided by Dellinger et al. (2015a) and calculate w^{Li}_{fluxes}, w^{Li}_{iso}, and $(Li/Al)_n$ (Al being the best insoluble element to normalise Li concentrations in solids; Dellinger et al., 2015a). As a matter of fact, there are several ways through which river mass budgets can be tested for being at equilibrium or not. Gaillardet et al. (1999), Dellinger et al. (2015a) solved the set of equilibrium river mass budget equations for the concentration of sediments in the river. Such "theoretical" or "predicted" sediment concentration would then be required for the river mass budget to be at equilibrium, and can be compared to a measured sediment concentration. Dellinger et al. (2015a) reported a good agreement between the predicted and the measured (either using sediment gauging or cosmogenic-nuclides derived estimates) river sediment concentration throughout the Amazon Basin, thus arguing in favor of an equilibrated river mass budget for Li and its isotopes in the Amazon.

Here, we re-visit this dataset using the framework developed in Appendix C for Ba but applied it to Li. We emphasize that this analysis simply consists in a reformulation of that previously used by Dellinger et al. (2015a). Following the same rationale as that developed in Appendix C (eqs. C1 to C6), the Li river mass budget is at equilibrium if:

$$1 = (Li/Al)_n + w^{Li} \tag{S.2}$$

with $(Li/Al)_n$ the Li/Al ratio of river sediment normalised to the same ratio for the Upper Continental Crust ratio (this ratio represents the degree of Li depletion in weathering-derived solids) and w^{Li} the proportion of riverine Li transported as dissolved species:

$$w^{Li}_{fluxes} = \frac{[Li]_{diss}}{[Li]_{diss} + [Li]_{spm} \times [spm]} \tag{S.3}$$

with $[Li]_{diss}$ and $[Li]_{spm}$ the Li abundance in the dissolved load (μg/L) and in suspended particulate matter (in mg/kg), respectively, and [spm] the concentration of river spm (in g/L).

In addition we can predict another estimate of w^{Li} using the partitioning of Li isotopes between the river dissolved and the solid fluxes, noted w^{Li}_{iso}, following the derivation from Bouchez et al. (2013):

$$w^{Li}_{iso} = \frac{\delta^{Li}_{rock} - \delta^{Li}_{sed}}{\delta^{Li}_{diss} - \delta^{Li}_{sed}} \tag{S.4}$$

with δ^{Li}_{rock}, δ^{Li}_{sed}, and δ^{Li}_{diss} the Li isotope composition of the weathered rock, the river suspended sediment and the dissolved load, respectively.

Consistently with results reported by Dellinger et al. (2015a), the Li river mass and isotope budgets suggest an equilibrium between supply to the Earth surface and riverine export in the Amazon Basin for Li. Importantly, Li is not a nutrient, which makes the contrast between the Li and Ba river mass budgets suggestive of the influence of biological cycling on Ba in the Amazon Basin.

References

Bouchez, J., Gaillardet, J., France-Lanord, C., Maurice, L., and Dutra-Maia, P. (2011). Grain size control of river suspended sediment geochemistry: Clues from amazon river depth profiles. *Geochemistry, Geophysics, Geosystems*, 12(3).

Bouchez, J., Gaillardet, J., Lupker, M., Louvat, P., France-Lanord, C., Maurice, L., Armijos, E., and Moquet, J.-S. (2012). Floodplains of large rivers: Weathering reactors or simple silos? *Chemical Geology*, 332:166–184.

Bouchez, J., von Blanckenburg, F., and Schuessler, J. A. (2013). Modeling novel stable isotope ratios in the weathering zone. *American Journal of Science*, 313(4):267–308.

Calmels, D., Gaillardet, J., and François, L. (2014). Sensitivity of carbonate weathering to soil Co_2 production by biological activity along a temperate climate transect. *Chemical Geology*, 390:74–86.

Dellinger, M., Bouchez, J., Gaillardet, J., and Faure, L. (2015a). Testing the steady state assumption for the Earth's surface denudation using Li isotopes in the Amazon Basin. *Procedia Earth and Planetary Science*, 13:162–168.

Dellinger, M., Gaillardet, J., Bouchez, J., Calmels, D., Louvat, P., Dosseto, A., Gorge, C., Alanoca, L., and Maurice, L. (2015b). Riverine Li isotope fractionation in the Amazon River basin controlled by the weathering regimes. *Geochimica et Cosmochimica Acta*, 164:71–93.

Dosseto, A., Bourdon, B., Gaillardet, J., Maurice-Bourgoin, L., and Allegre, C. J. (2006). Weathering and transport of sediments in the Bolivian andes: Time constraints from uranium-series isotopes. *Earth and Planetary Science Letters*, 248(3-4):759–771.

Edmond, J., Palmer, M., Measures, C., Grant, B., and Stallard, R. (1995). The fluvial geochemistry and denudation rate of the Guayana Shield in Venezuela, Colombia, and Brazil. *Geochimica et Cosmochimica Acta*, 59(16):3301–3325.

Gaillardet, J., Dupré, B., and Allègre, C. J. (1995). A global geochemical mass budget applied to the Congo Basin rivers: erosion rates and continental crust composition. *Geochimica et Cosmochimica Acta*, 59(17):3469–3485.

Gaillardet, J., Dupré, B., and Allègre, C. J. (1999). Geochemistry of large river suspended sediments: silicate weathering or recycling tracer? *Geochimica et Cosmochimica Acta*, 63(23-24):4037–4051.

Jung, M., Koirala, S., Weber, U., Ichii, K., Gans, F., Camps-Valls, G., Papale, D., Schwalm, C., Tramontana, G., and Reichstein, M. (2019). The FLUXCOM ensemble of global land-atmosphere energy fluxes. *Scientific data*, 6(1):74.

Li, S.-L., Calmels, D., Han, G., Gaillardet, J., and Liu, C.-Q. (2008). Sulfuric acid as an agent of carbonate weathering constrained by $\delta^{13}C_{DIC}$: Examples from Southwest China. *Earth and Planetary Science Letters*, 270(3-4):189–199.

Louvat, P. (1997). *Etude géochimique de l'érosion fluviale d'îles volcaniques à l'aide des bilans d'éléments majeurs et traces*. PhD thesis, Institut de physique du globe (Paris).

Louvat, P. and Allègre, C. J. (1997). Present denudation rates on the island of Reunion determined by river geochemistry: basalt weathering and mass budget between chemical and mechanical erosions. *Geochimica et Cosmochimica Acta*, 61(17):3645–3669.

Louvat, P., Gislason, S. R., and Allègre, C. J. (2008). Chemical and mechanical erosion rates in Iceland as deduced from river dissolved and solid material. *American Journal of Science*, 308(5):679–726.

Millot, R., Gaillardet, J., Dupré, B., and Allègre, C. J. (2002). The global control of silicate weathering rates and the coupling with physical erosion: new insights from rivers of the canadian shield. *Earth and Planetary Science Letters*, 196(1-2):83–98.

Millot, R., Gaillardet, J., Dupré, B., and Allègre, C. J. (2003). Northern latitude chemical weathering rates: clues from the mackenzie river basin, canada. *Geochimica et Cosmochimica Acta*, 67(7):1305–1329.

Tramontana, G., Jung, M., Camps-Valls, G., Ichii, K., Ráduly, B., Reichstein, M., Schwalm, C. R., Arain, M. A., Cescatti, A., Kiely, G., et al. (2016). Predicting carbon dioxide and energy fluxes across global fluxnet sites with regression algorithms. *Biogeosciences Discussions*.

Supplementary figures

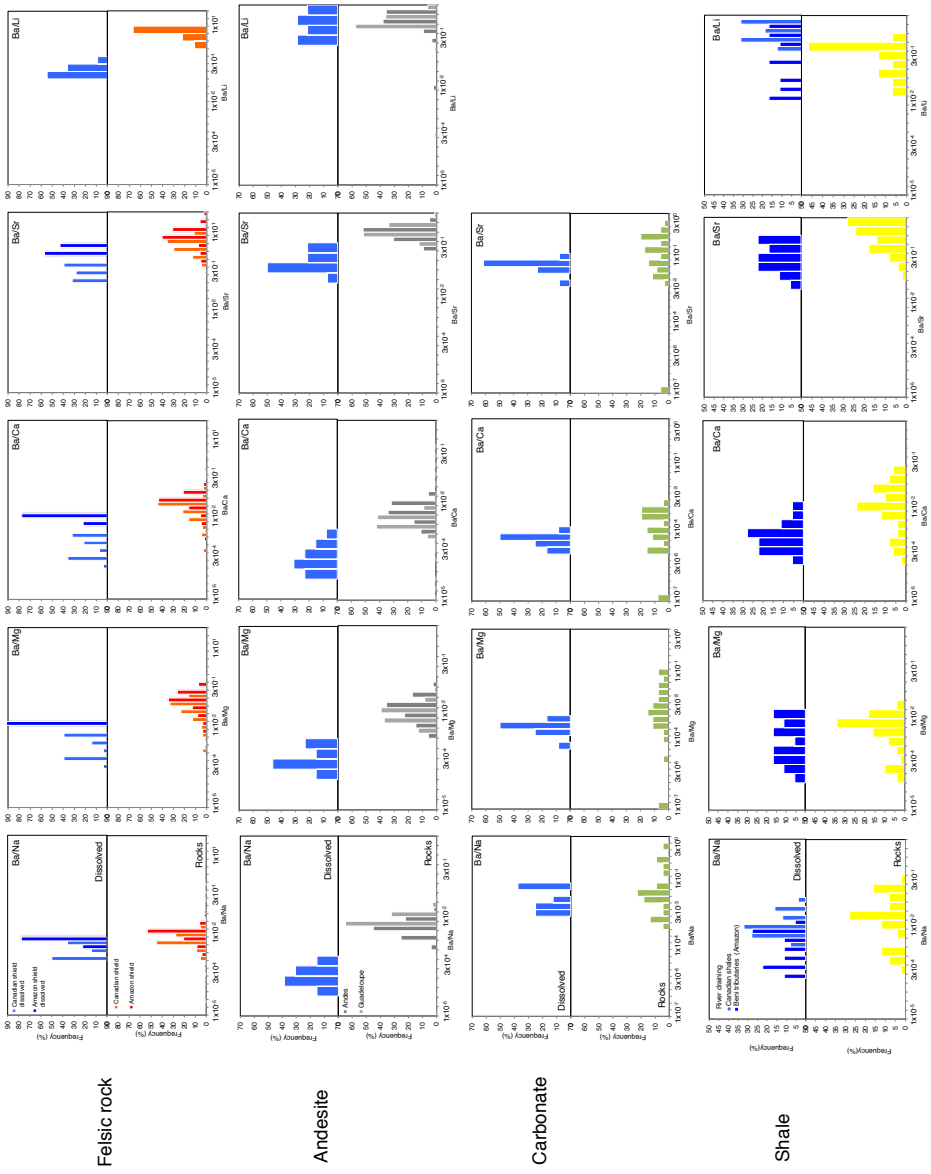

Figure S1. Histograms of Ba/X ratios (X = Na, Ca, Mg, Sr, Li) of the dissolved load of rivers draining monolithological basin, and of the corresponding rocks established from worldwide compilations. Igneous rock (felsic and andesite) and carbonate data are derived from GEOROC (http://georoc.mpch-mainz.gwdg.de/georoc/), and shale data are derived from both GEOROC and our own measurements (all data are presented in repository doi:10.5281/zenodo.4050339). River chemical composition data are derived from a series of studies published by the IPGP group for carbonates (Li et al., 2008; Calmels et al., 2014), andesites, shales (Millot et al., 2003; Dosseto et al., 2006), for some of the felsic igneous rocks (Millot et al., 2002), and for for basalts (Louvat and Allègre, 1997; Louvat, 1997; Louvat et al., 2008) augmented by new data. The other part of the data is taken from Edmond et al. (1995). For each rock type, we calculate a median and the corresponding uncertainty calculated as 2 S.D. /$\sqrt{N}$ with N = 1685 for Andean andesites, N = 50 for shales and N = 149 for felsic igneous rocks where the values are used in eq. B1.

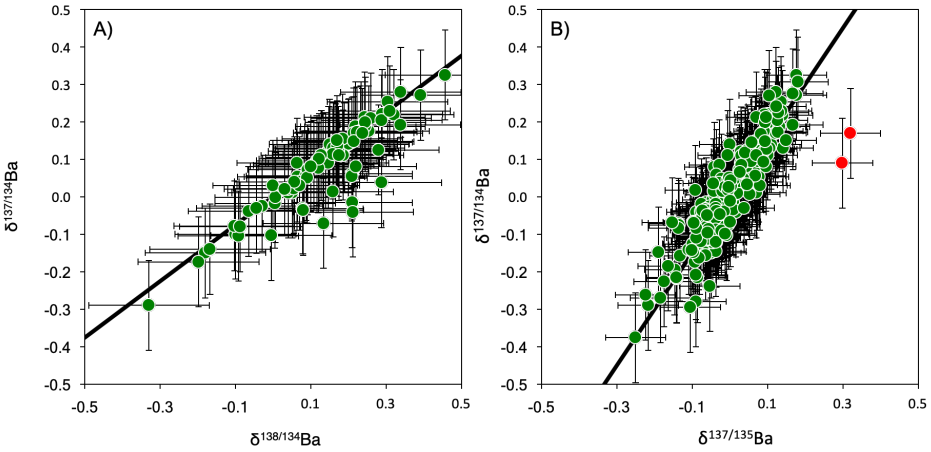

Figure S2. (A) $\delta^{137/134}$Ba *vs* $\delta^{138/134}$Ba for dissolved samples, which should be Ce and La-free (B) $\delta^{137/134}$Ba *vs* $\delta^{137/135}$Ba for all samples. Mass-dependent fractionation is represented by the black line. Each dot is a single measurement and the error bars represent the 2 S.D. on the long-term measurements of our reference materials (Babe27 and JB-2). The two red dots are not mass-dependent for $\delta^{137/135}$Ba, however other single measurements of these samples shows the same values and displays mass dependent fractionation; for this reasons we do not dissmiss these data.

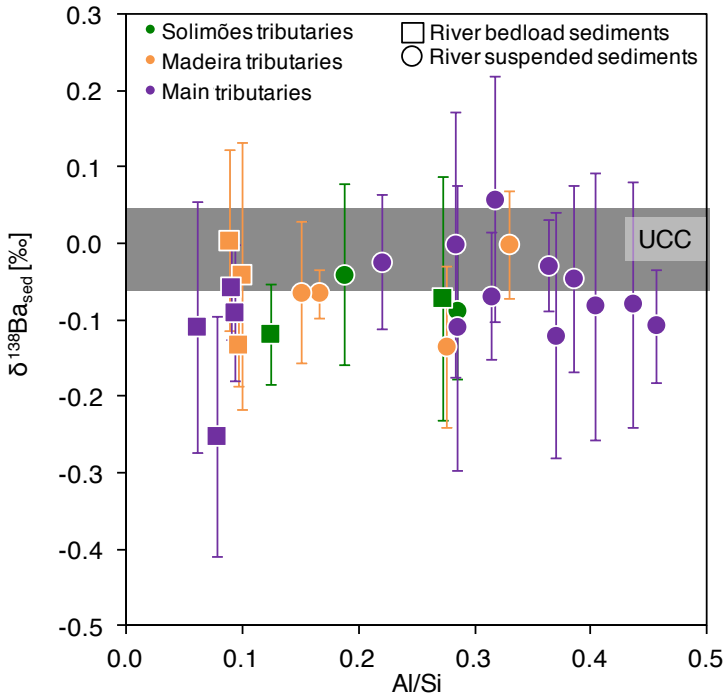

Figure S3. δ^{138}Ba of river sediments in the Amazon Basin as a function of their Al/Si ratio, used here as a tracer for sediment grain size (Bouchez et al., 2011).

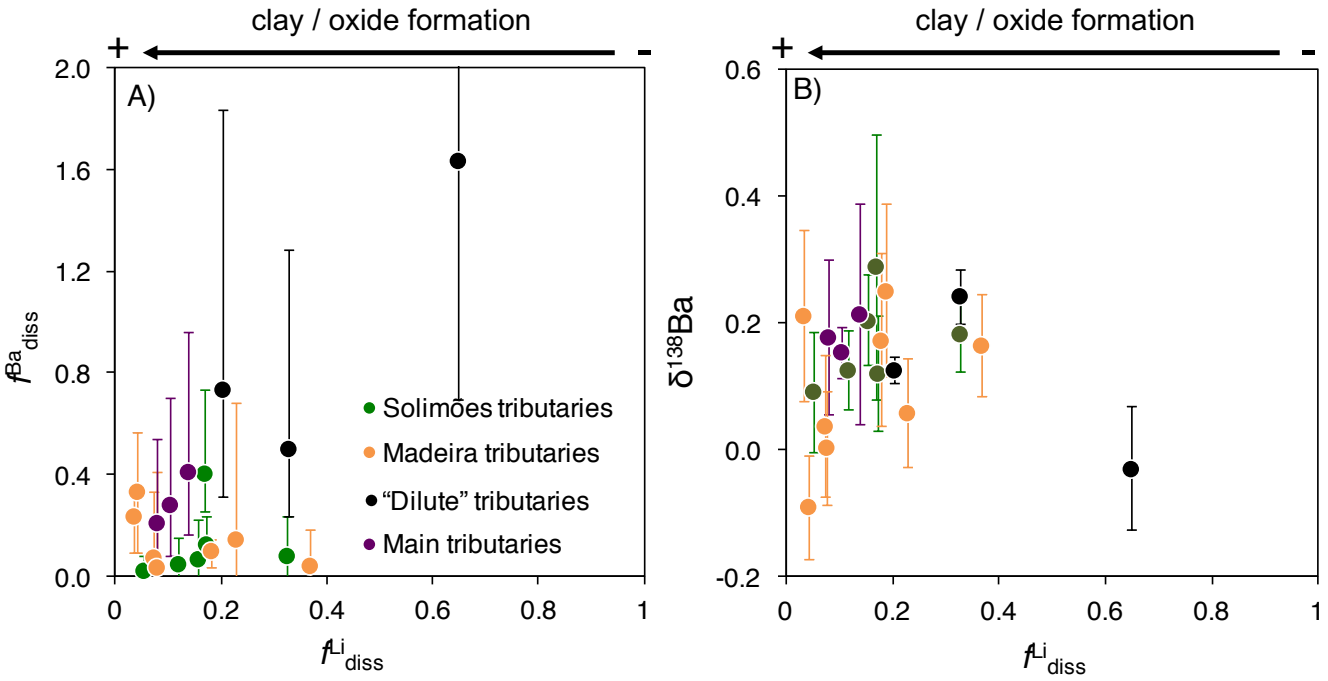

Figure S4. A) f^{Ba}_{diss} *vs* f^{Li}_{diss} and B) δ^{138}Ba *vs* f^{Li}_{diss}, used to test the potential control of river dissolved Ba isotope composition by secondary phase formation: f^{Li}_{diss} is the fraction of the Li "initially" released from rock dissolution that remains in solution after formation of secondary phases such as (hydr)oxydes and clays; f^{Li}_{diss} is thus an index for clay/oxyde formation.

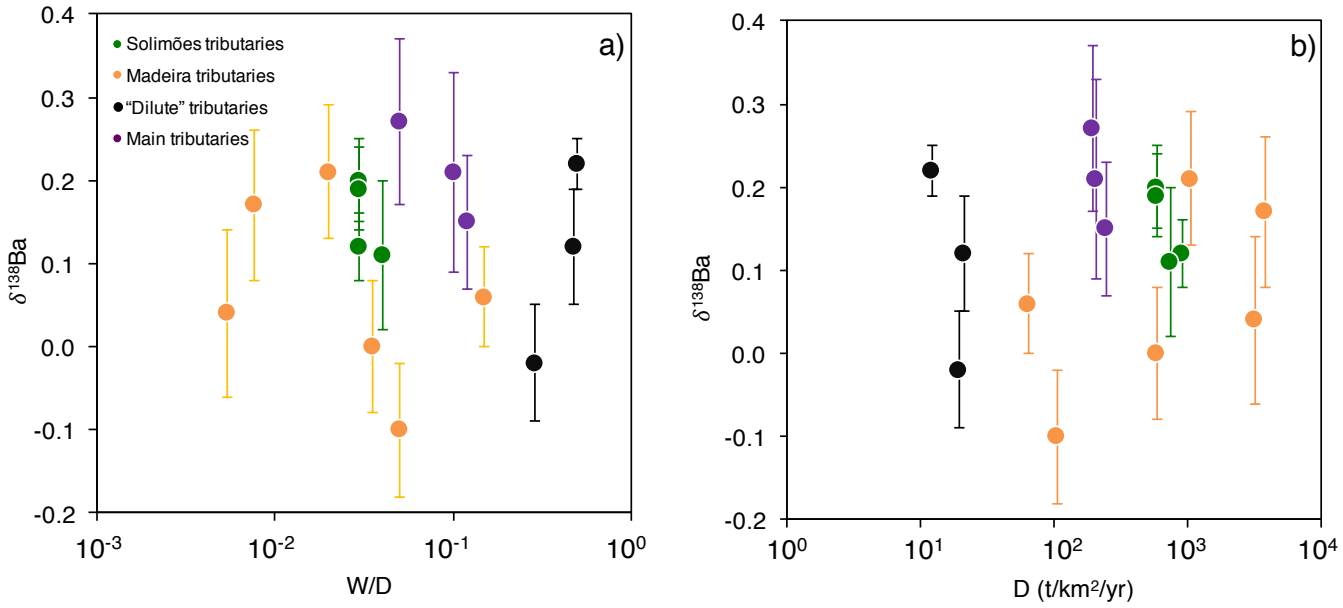

Figure S5. Dissolved Ba isotope composition in the Amazon Basin *vs.* (a) the W/D ratio (weathering intensity) and (b) D (denudation rate).

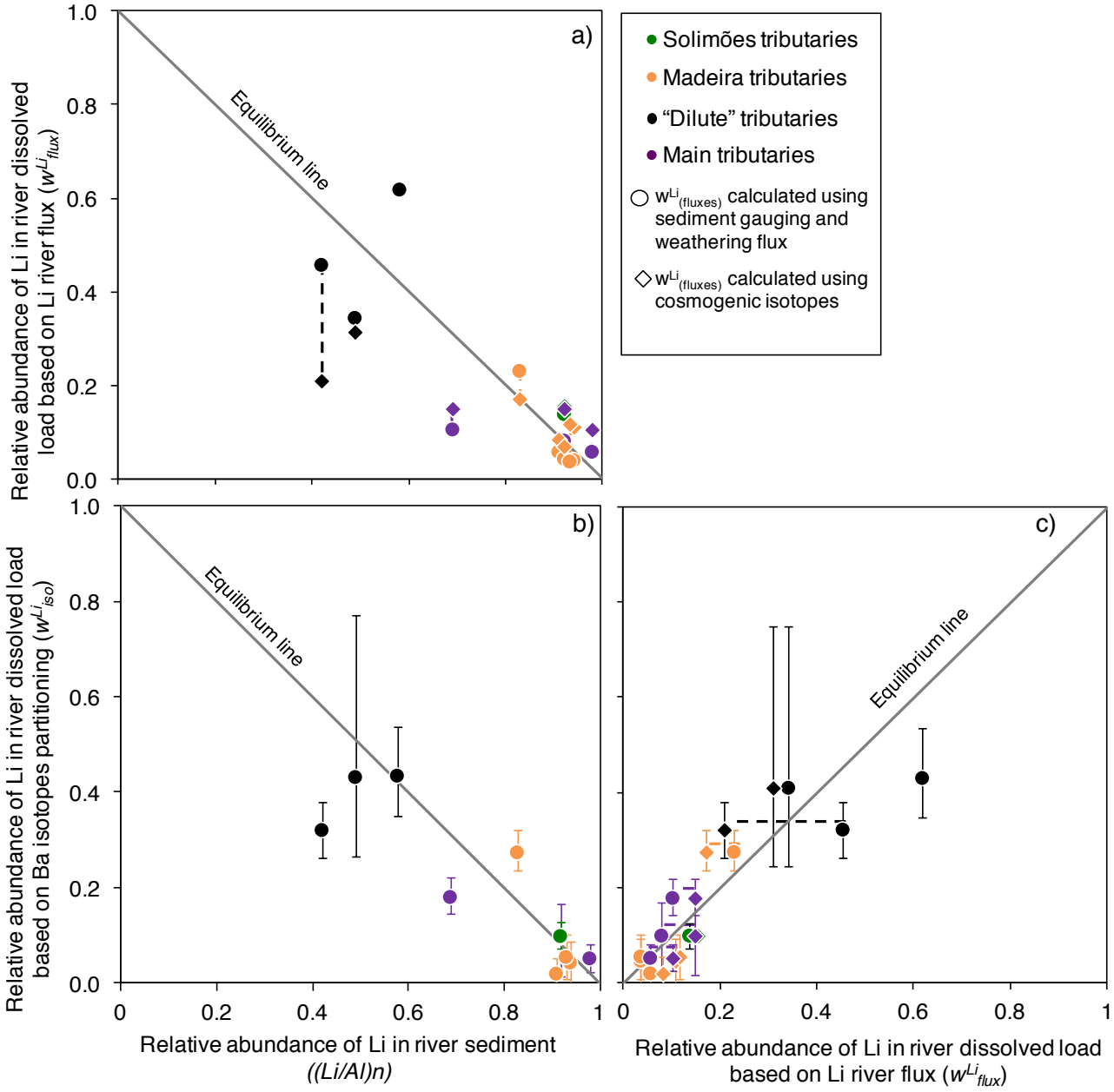

Figure S6. Test for the equilibrium of the river mass budget of Li in the Amazon Basin using elemental (eqs. S.3 and S.2) and isotopic (eq. S.4) ratios. Uncertainties on w^{Li}_{fluxes} stem from the two ways this parameter can be calculated (river gauging and cosmogenic nuclides; see text for details). Uncertainties on w^{Li}_{iso} have been evaluated using Monte Carlo error propagation based on the uncertainties on individual parameters in eq. S.4, and are shown here as 68%CI.

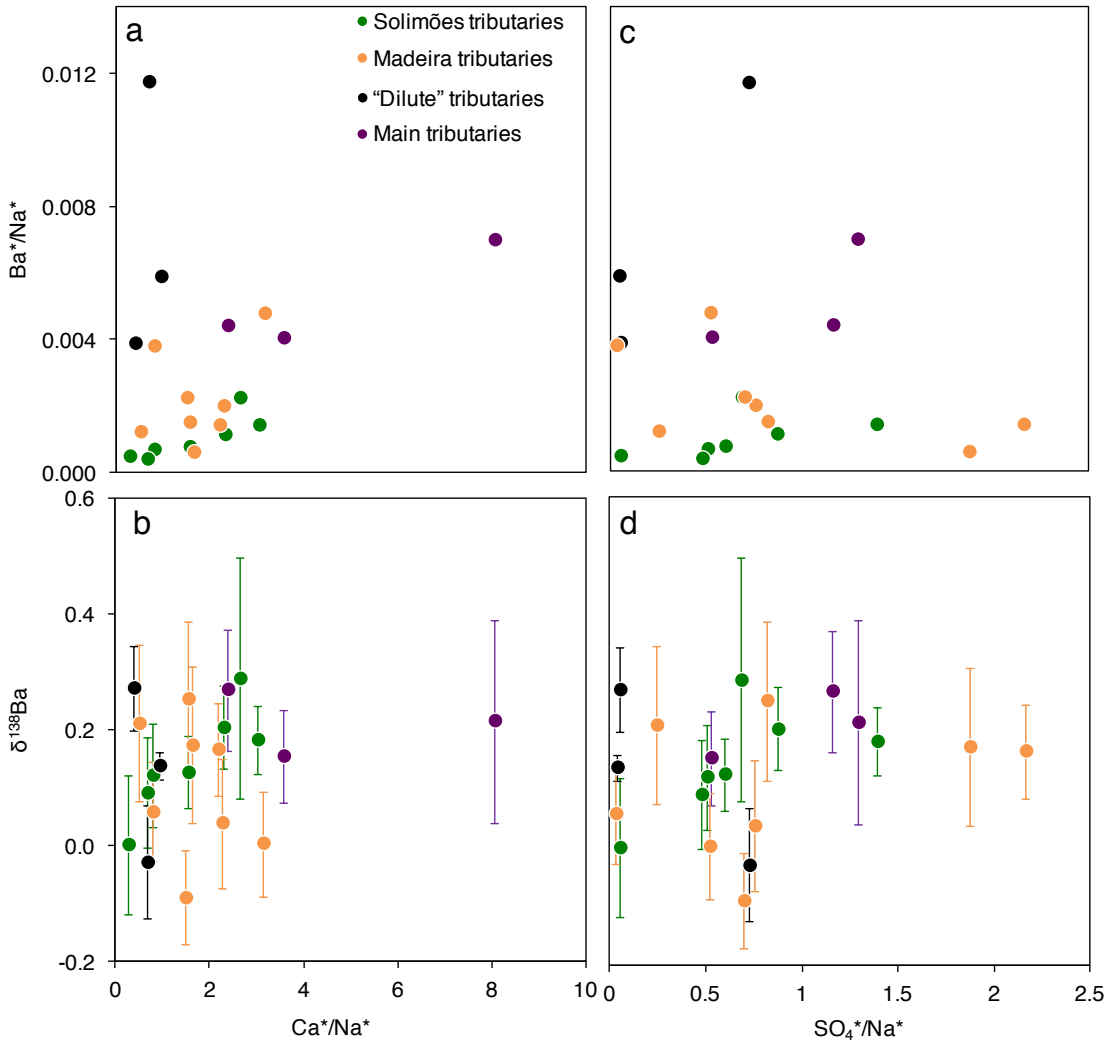

Figure S7. Scatter plots of Ba*/Na* and δ^{138}Ba *vs* Ca*/Na*, SO_4/Na*, for the dissolved load of the Amazon rivers ("*" refers to dissolved concentrations corrected from rain-derived inputs).